Maximally Random Discrete-Spin Systems with Symmetric and Asymmetric Interactions and Maximally Degenerate Ordering

Bora Atalay[1] and A. Nihat Berker[2,3]

[1] *Faculty of Engineering and Natural Sciences, Sabancı University, Tuzla, Istanbul 34956, Turkey*
[2] *Faculty of Engineering and Natural Sciences, Kadir Has University, Cibali, Istanbul 34083, Turkey*
[3] *Department of Physics, Massachusetts Institute of Technology, Cambridge, Massachusetts 02139, USA*

Discrete-spin systems with maximally random nearest-neighbor interactions that can be symmetric or asymmetric, ferromagnetic or antiferromagnetic, including off-diagonal disorder, are studied, for the number of states $q = 3, 4$ in d dimensions. We use renormalization-group theory that is exact for hierarchical lattices and approximate (Migdal-Kadanoff) for hypercubic lattices. For all $d > 1$ and all non-infinite temperatures, the system eventually renormalizes to a random single state, thus signaling $q \times q$ degenerate ordering. Note that this is the maximally degenerate ordering. For high-temperature initial conditions, the system crosses over to this highly degenerate ordering only after spending many renormalization-group iterations near the disordered (infinite-temperature) fixed point. Thus, a temperature range of short-range disorder in the presence of long-range order is identified, as previously seen in underfrustrated Ising spin-glass systems. The entropy is calculated for all temperatures, behaves similarly for ferromagnetic and antiferromagnetic interactions, and shows a derivative maximum at the short-range disordering temperature. With a sharp immediate contrast of infinitesimally higher dimension $1 + \epsilon$, the system is as expected disordered at all temperatures for $d = 1$.

PACS numbers: 75.10.Nr, 05.10.Cc, 64.60.De, 75.50.Lk

I. INTRODUCTION: ASYMMETRIC AND SYMMETRIC MAXIMALLY RANDOM SPIN MODELS

Spin models such as Ising, Potts, ice models show a richness of phase transitions and multicritical phenomena [1, 2] that is qualitatively compounded with the addition of frozen (quenched) randomness. Examples are the emerging chaos in spin glasses with competing ferromagnetic and antiferromagnetic (and more recently, without recourse to ferromagnetism vs. antiferromagnetism, competing left and right chiral [3]) interactions, the conversion of first-order phase transitions to second-order phase transitions, and the infinite multitude of accumulating phases as devil's staircases. In the current study, frozen randomness is taken to the limit, in $q = 3, 4$ state models in arbitrary dimension d and the results are quite unexpected.

The systems that we study are quenched maximally random q-state discrete spin models with nearest-neighbor interactions, with Hamiltonian

$$-\beta\mathcal{H} = -\sum_{\langle ij\rangle} \beta\mathcal{H}_{ij}, \tag{1}$$

where the sum is over nearest-neighbor pairs of sites $< ij >$. The maximal randomness is best expressed in the transfer matrix T_{ij}, e.g., for $q = 3$,

$$\mathbf{T}_{ij} \equiv e^{-\beta\mathcal{H}_{ij}} = \left(\begin{array}{ccc} 1 & e^J & 1 \\ 1 & 1 & e^J \\ e^J & 1 & 1 \end{array}\right), \left(\begin{array}{ccc} 1 & 1 & e^J \\ e^J & 1 & 1 \\ 1 & e^J & 1 \end{array}\right), \left(\begin{array}{ccc} e^J & 1 & 1 \\ 1 & 1 & e^J \\ 1 & e^J & 1 \end{array}\right), \left(\begin{array}{ccc} 1 & 1 & e^J \\ 1 & e^J & 1 \\ e^J & 1 & 1 \end{array}\right), \left(\begin{array}{ccc} 1 & e^J & 1 \\ e^J & 1 & 1 \\ 1 & 1 & e^J \end{array}\right), \text{ or } \left(\begin{array}{ccc} e^J & 1 & 1 \\ 1 & e^J & 1 \\ 1 & 1 & e^J \end{array}\right), \tag{2}$$

where each row and each column has, randomly, a single e^J element, so that there are 6 such possibilities (for $q = 4$, also studied here, there are 24 such possibilities), and $J > 0$ or $J < 0$ respectively for ferromagnetic or antiferromagnetic interactions, both of which are treated in this study. Under renormalization-group transformation, all elements of the transfer matrices across the system randomize. The first two possible transfer matrices on the right side of Eq. (1) represent asymmetric interaction, in the sense that the nearest-neighbor states $(s_i, s_j) = (a, b)$ and (b, a) have different energies, where $s_i = a, b,$ or c are the $q = 3$ possible states of a given site i. Asymmetric interactions occur in neural network systems [4] and are largely unexplored in statistical mechanics. On the other hand, the last four possible transfer matrices on the right side of Eq. (1) exemplify symmetric interaction, the nearest-neighbor states $(s_i, s_j) = (a, b)$ and (b, a) having the same energies. As also explained below, even when starting with only symmetric interactions (the last four matrices), asymmetric interactions are generated under renormalization-group transformations and the same ordering results are obtained. The

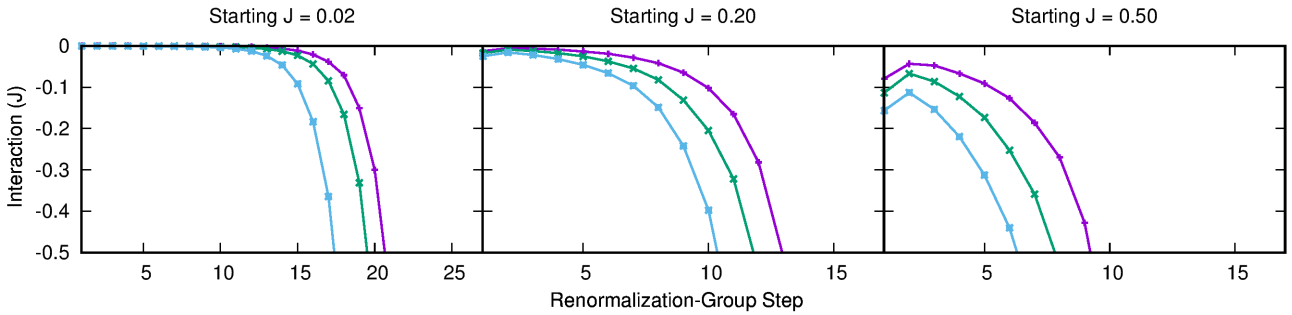

FIG. 1. Renormalization-group trajectories for the system with $q = 3$ states in $d = 3$ dimensions, starting at three different temperatures $T = J^{-1}$. Shown are the second (J_2), third (J_3) largest energies and the matrix average of the eight non-leading energies ($< J_{2-9} >$) of the transfer matrix, averaged over the quenched random distribution. The leading energy is $J_1 = 0$ by subtractive choice. Starting at any non-zero temperature, the system renormalizes to a state in which the leading energy is totally dominant, all other energies renormalizing to $-\infty$. The matrix position of the single asymptotically dominant element occurs randomly among the $q \times q$ possibilities including off-diagonal and therefore necessarily asymmetric, but is the same across the quenched random distribution. However, starting at high temperatures, as seen e.g. in the left and center panels in this figure, the system spends many renormalization-group iterations near the infinite-temperature fixed point (where all energies are zero), before crossing over to the ordered fixed point. This signifies short-range disorder, in the presence of long-range order, as also reflected in the specific heat peaks caused by short-range disordering.

generalization of the above model to arbitrary q is obvious.

II. RENORMALIZATION-GROUP TRANSFORMATION

The renormalization-group method is readily implemented to the transfer matrix form of the interactions. The quenched randomness aspect of the problem is included by randomly creating 500 transfer matrices from the 6 possibilities of Eq. (1) and perpetuating these random 500 transfer matrices throughout the renormalization-group steps given below. Note that we start with a single initial value of J, which is proportional to the inverse temperature. Quenched randomness comes from the positioning within the matrix. Under renormalization-group transformation, each matrix element evolves quantitively quenched randomly.

The renormalization-group transformation begins by the "bond-moving" step in which b^{d-1} transfer matrices, each randomly chosen from the 500, have their corresponding matrix elements multiplied. This operation is repeated 500 times, thus generating 500 new transfer matrices. The final, "decimation" step of the renormalization-group transformation is the matrix multiplication of b transfer matrices, again each randomly chosen from the 500. This operation is also repeated 500 times, again generating 500 renormalized transfer matrices. The length rescaling factor is taken as $b = 2$ in our calculation. At each transfer-matrix calculation above, each element of the resulting transfer matrix is divided by the largest element, resulting in a matrix with the largest element being unity. This does not affect the physics, since it corresponds to subtracting a constant from the Hamiltonian. These subtractive constants (the natural logarithm of the dividing element) are scale-accumulated, as explained below, for the calculation of entropy.

The above transformation is the approximate Migdal-Kadanoff [5, 6] renormalization-group transformation for hypercubic lattices and, simultaneously, the exact renormalization-group transformation of a hierarchical lattice [7–9]. This procedure has been explained in detail in previous works.[3] For most recent exact calculations on hierarchical lattices, see Ref.[10–15], including finance [16] and DNA-binding [17] problems.

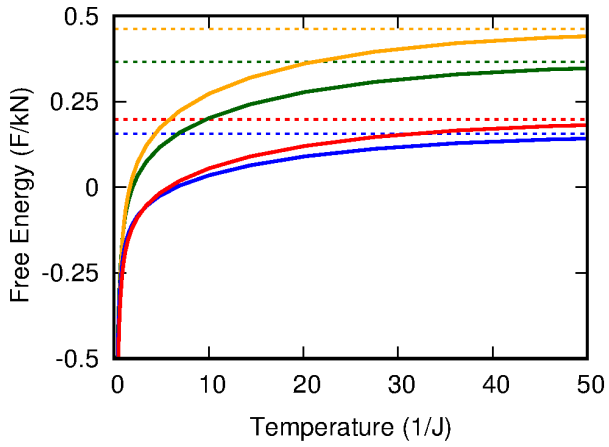

FIG. 2. Calculated free energy per bond as a function of temperature $T = J^{-1}$. The curves are, from top to bottom, for $(q = 4, d = 2), (q = 3, d = 2), (q = 4, d = 3), (q = 3, d = 3)$. The expected $T = \infty$ values of $f = F/kN = \ln q/(b^d - 1)$ are given by the dashed lines and match the calculations.

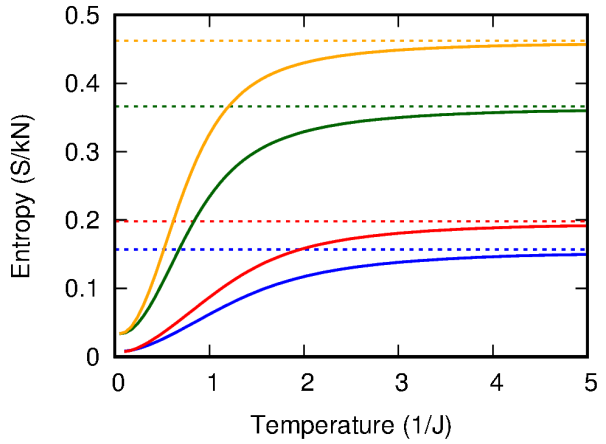

FIG. 3. Calculated entropy per bond as a function of temperature $T = J^{-1}$, for $q = 3, 4$ states in $d = 3, 4$ dimensions. The curves are, from top to bottom, for $(q = 4, d = 2), (q = 3, d = 2), (q = 4, d = 3), (q = 3, d = 3)$. The expected $T = \infty$ values of $S/kN = \ln q/(b^d - 1)$ are given by the dashed lines and match the calculations.

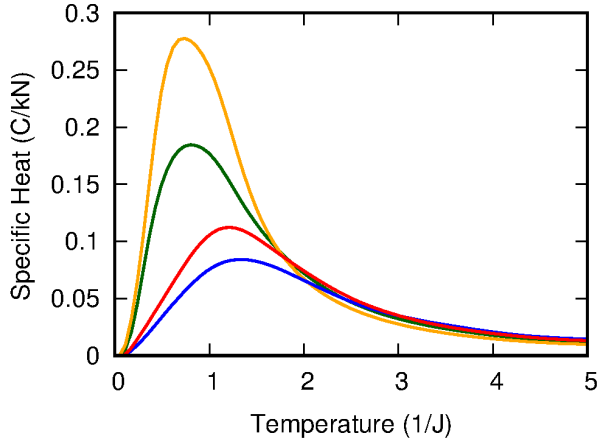

FIG. 4. Calculated specific heat as a function of temperature $T = J^{-1}$, for $q = 3, 4$ states in $d = 3, 4$ dimensions. The curves are, from top to bottom, for $(q = 4, d = 2), (q = 3, d = 2), (q = 4, d = 3), (q = 3, d = 3)$. A specific heat maximum occurs at short-range disordering.

III. ASYMPTOTICALLY DOMINANT ALL-TEMPERATURE FREEZING IN $d > 1$ WITH HIGH-TEMPERATURE SHORT-RANGE DISORDERING

Figure 1 shows the renormalization-group trajectories for the system with $q = 3$ states in $d = 3$ dimensions, starting at three different temperatures $T = J^{-1}$. Shown are the second (J_2), third (J_3) largest energies and the matrix average of the eight non-leading energies ($< J_{2-9} >$) of the transfer matrix, averaged over the quenched random distribution, namely

$$J_{ij} = \ln(T_{ij}), \tag{3}$$

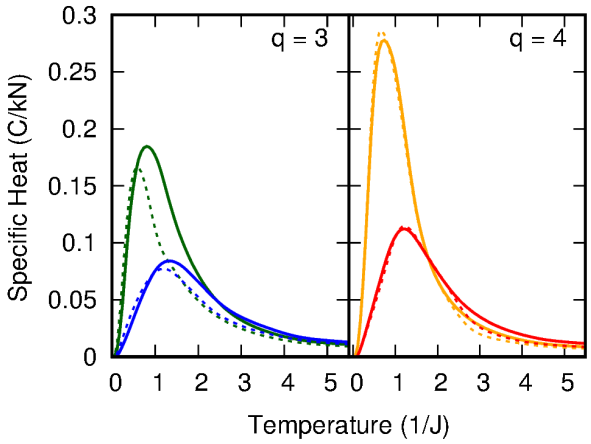

FIG. 5. Calculated specific heat as a function of temperature $T = |J|^{-1}$ for ferromagnetic ($J > 0$), full curves, and antiferromagnetic ($J < 0$), dashed curves, systems, for $q = 3, 4$ states in $d = 3, 4$ dimensions. The curves are, from top to bottom in each panel, for $d = 2$ and $d = 3$. The quantitatively same short-range disordering behavior is seen for both ferromagnetic and antiferromagnetic systems.

for each of the elements of the $q \times q$ transfer matrix. The leading energy is $J_1 = 0$ by subtractive overall constant, as explained above. As seen in this figure, starting at low temperature $T = 2$, the system renormalizes to a state in which the leading energy is totally dominant, all other energies renormalizing to $-\infty$. The matrix position of the single asymptotically dominant element occurs randomly among the $q \times q$ possibilities including off-diagonal and therefore necessarily asymmetric, but is the same across the quenched random distribution. However, starting at high temperatures, as seen e.g. in the left and center panels of Fig. 1, the system spends many renormalization-group iterations near the infinite-temperature fixed point (where all energies are zero), before crossing over to the ordered fixed point. This signifies short-range disorder, in the presence of long-range order, as also reflected in the specific heat peaks caused by short-range disordering as discussed below. A similar smeared transition to short-range disorder in the presence of long-range order has previously been seen in underfrustrated Ising spin-glass systems.[18]

IV. FREE ENERGY, ENTROPY, AND SPECIFIC HEAT

The renormalization-group solution gives the complete equilibrium thermodynamics for the systems studied. The dimensionless free energy per bond $f = F/kN$ is obtained by summing the additive constants generated at each renormalization-group step,

$$f = \frac{1}{N} \ln \sum_{\{s_i\}} e^{-\beta \mathcal{H}} = \sum_{n=1} \frac{G^{(n)}}{b^{dn}}, \tag{4}$$

where N is the number of bonds in the initial unrenormalized system, the first sum is over all states of the system, the second sum is over all renormalization-group steps n, $G^{(n)}$ is the additive constant generated at the (n)th renormalization-group transformation averaged over the quenched random distribution, and the sum quickly converges numerically.

From the dimensionless free energy per bond f, the entropy per bond S/kN is calculated as

$$\frac{S}{kN} = f - J\frac{\partial f}{\partial J} \tag{5}$$

and the specific heat C/kN is calculated as

$$\frac{C}{kN} = T\frac{\partial(S/kN)}{\partial T} = -J\frac{\partial(S/kN)}{\partial J}\,. \tag{6}$$

Figures 2-4 give the calculated free energies f, entropies S/kN, and specific heats C/kN per bond as functions of temperature $T = J^{-1}$, for $q = 3, 4$ states in $d = 3, 4$ dimensions. The expected $T = \infty$ values of $f = \ln q/(b^d - 1)$ and $S/kN = \ln q/(b^d - 1)$ are given by the dashed lines and match the calculations. A specific heat maximum occurs at the temperature of the short-range disordering.

V. ANTIFERROMAGNETIC MAXIMALLY RANDOM SYSTEMS

We have repeated our calculations for antiferromagnetic ($J < 0$) systems and obtained quantitatively similar behavior. Figs. 5 shows the calculated specific heats as a function of temperature $T = |J|^{-1}$ for ferromagnetic ($J > 0$) and antiferromagnetic ($J < 0$) systems, for $q = 3, 4$ states in $d = 3, 4$ dimensions. The full-temperature range ($T < -\infty$) maximally degenerate long-range ordering and a quantitatively same short-range disordering at high temperature is seen for both ferromagnetic and antiferromagnetic systems.

VI. CONCLUSION

We have studied maximally random discrete-spin systems with symmetric and asymmetric interactions and have found, quite surprisingly, (1) quenched random long-range order at all non-infinite temperatures for $d > 1$, (2) short-range disordering at high temperatures, via a smeared transition and a specific-heat peak, while sustaining long-range order. The latter behavior has also been seen in underfrustrated Ising spin-glass systems.[18]

ACKNOWLEDGMENTS

Support by the Academy of Sciences of Turkey (TÜBA) is gratefully acknowledged. We thank Tolga Çağlar for most useful discussions.

[1] B. Nienhuis, A. N. Berker, E. K. Riedel, and M. Schick, Phys. Rev. Let. **43**, 737 (1979).
[2] G. Delfino and E. Tartaglia, Phys. Rev. E **96**, 042137 (2017).
[3] T. Çağlar and A. N. Berker, Phys. Rev. E **96**, 032103 (2017).
[4] E. Domany, J. L. van Hemmen, and K. Schulten (Eds.) *Models of Neural Networks* (Springer-Verlag, Berlin, 1991).
[5] A. A. Migdal, Zh. Eksp. Teor. Fiz. **69**, 1457 (1975) [Sov. Phys. JETP **42**, 743 (1976)].
[6] L. P. Kadanoff, Ann. Phys. (N.Y.) **100**, 359 (1976).
[7] A. N. Berker and S. Ostlund, J. Phys. C **12**, 4961 (1979).
[8] R. B. Griffiths and M. Kaufman, Phys. Rev. B **26**, 5022R (1982).
[9] M. Kaufman and R. B. Griffiths, Phys. Rev. B **30**, 244 (1984).
[10] N. Masuda, M. A. Porter, and R. Lambiotte, Phys. Repts. **716**, 1 (2017).
[11] S. Li and S. Boettcher, Phys. Rev. A **95**, 032301 (2017).
[12] P. Bleher, M. Lyubich, and R. Roeder, J. Mathematiques Pures et Appliquées **107**, 491 (2017).
[13] H. Li and Z. Zhang, Theoretical Comp. Sci. **675**, 64 (2017).
[14] J. Peng and E. Agliari, Chaos **27** 083108 (2017).
[15] T. Nogawa, arXiv:1710.04014 [cond-mat.stat-mech](2017)
[16] S. J. Sirca and M. Omladic, ARS Mathematica Contemporanea **13**, 63 (2017).
[17] J. Maji, F. Seno, A. Trovato, and S. M. Bhattacharjee, J. Stat. Mech.: Theory Exp. 073203 (2017).
[18] E. Ilker and A. N. Berker, Phys. Rev. E **89**, 042139 (2014).